# Varying relationships between fire intensity and fire size at global scale

Pierre Laurent[1], Florent Mouillot[2], Maria Vanesa Moreno[2], Chao Yue[1], Philippe Ciais[1]

[1]Laboratoire des Sciences du Climat et de l'Environnement (LSCE), CEA-CNRS-UVSQ, UMR8212, Gif-sur-Yvette, France
[2]UMR CEFE 5175, Centre National de la Recherche Scientifique (CNRS), Université de Montpellier, Université Paul-Valéry Montpellier, Ecole Pratique des Hautes Etudes (EPHE), Institut de Recherche pour le Développement, 1919 route de Mende, 34293 Montpellier CEDEX 5, France

*Correspondence to*: Pierre Laurent (**pierre.laurent@ipsl.lsce.fr**), Florent Mouillot (**florent.mouillet@cefe.cnrs.fr**)

**Abstract.** Vegetation fires are an important process in the Earth system. Fire intensity locally impacts fuel consumption, damage to the vegetation, chemical composition of fire emissions but also how fires spread across landscapes. It has been observed that fire occurrence, defined as the frequency of active fires detected by the MODIS sensor, is related to intensity with a hump-shaped empirical relation meaning that occurrence reaches a maximum at intermediate intensity. Raw burned area products obtained from remote-sensing can not discriminate between ignition and propagation processes. Here we use the newly delivered global FRY database, which provides fire patch functional traits including fire patch size from satellite observation, to go beyond burned area, and to test if fire size is driven by fire intensity at global scale as expected from empirical fire spread models. We show that in most regions of the world the linear relationship between fire intensity and fire patch size saturates for a threshold of intermediate intensity fires. The value of the threshold differs from one region to another, and we suggest that it might be driven by drought, and the amount of available biomass. In some regions, once this threshold is reached, we also observe that fire size decreases for the most intense fires, which mostly happen in the late fire season. According to the percolation theory, we suggest that this effect is a consequence of the increasing fragmentation of fuel continuity along the fire season so that landscape-scale feedbacks should be developed in global fire modules.

## 1 Introduction

Fire is a major perturbation of the Earth system, which impacts the biomass distribution and vegetation structure, the carbon cycle, global atmospheric chemistry, air quality and climate (Bowman et al. 2009). Fire is therefore recognized as an essential climatic variable (GCOS 2011), and the potential impact of global warming on drought severity and fire season length is an important research topic (Flannigan et al. 2009, Krawchuk et al. 2009, Aragão et al. 2018). As a result, most Dynamic Global Vegetation Models (DGVMs) have included fire modules (see Hantson et al. 2016, Rabin et al. 2017 for a review) to provide reliable prediction of vegetation dynamics. Substantial efforts have been devoted in the past decades to create reliable global burned area, active fires and fire intensity global datasets which allow to quantify the fire perturbation since the beginning of the 2000's (Mouillot et al. 2014) and for benchmarking of DGVMs fire modules.

A fire can be decomposed as a two-step process, the ignition and the propagation (Pyne 1996, Scott et al. 2014). Potential fire ignitions are set by lightning strikes and humans (deliberately or accidentally), and the probability that an ignition turns into a spreading fire event mainly depends on fuel type and its moisture content at the location of the ignition. The Rothermel's equation (Wagner 1969, Rothermel 1972) has long been used to model fire propagation in landscape fire succession models (Cary et al. 2006), whose rate of spread scales with a power function of the wind velocity, landscape slope and fire intensity. However, this model, used in most DGVM processed-based fire modules, has only been benchmarked on experimental and localized fires, discarding topographic and landscape effects. However, for larger natural fires, the continuity of the fuel bed also has an impact on fire propagation: a homogeneous fuel bed usually promotes fire propagation (Baker et al. 1994) while fragmented landscape with a heterogeneity of fuel patches reduces fire spread (Turner et al. 1989). On the other hand, the velocity of fire propagation determines the amount of fuel entering the combustion zone, and therefore feeds back on the intensity of the fire event. In addition to its coupling with fire propagation, fire intensity also significantly impacts the fuel combustion completeness (Crutzen et al. 1979), the chemical composition of the emissions (Tang et al. 2017), the amplitude and severity of vegetation damage and its post-fire regeneration ability (Bond and Keeley et al. 2005). As a result, analyses focusing on fire patches rather than on raw burn area have emerged in the last decade in order to study the fire patch size distribution (Archibald et al. 2010, Hantson et al. 2015, Laurent et al. 2018) or as a tool to map the different fire regimes at global scale (Archibald et al. 2013).

Recent studies (Pausas and Ribeiro et al. 2013, Luo et al. 2017) have shown that fire occurrence, defined as the number of remotely detected active fires in unit of time per unit area, increases with fire intensity up until a threshold is reached (so-called Intermediate Fire Occurrence-Intensity (IFOI) hypothesis) above which occurrence decreases with increasing intensity. Since ignition and propagation are different processes and are not driven by the same climatic variables, it is necessary to go beyond fire occurrence and burned area and to consider individual fire events. Here we document and investigate the relationship between fire patch size derived from BA data and fire radiative power (FRP) at global scale based on remote sensing information. FRP measures the energy emitted through radiative processes released during combustion, and can be associated with fire intensity (Wooster et al. 2005, Ichoku et al. 2008, Barrett and Kasischke 2013, Wooster et al. 2013). A positive relationship between fire patch size and fire intensity is expected from the Rothermel's equation at least for small fire size, but we do not know if this holds up at global and regional scale and for bigger fires : where landscape fragmentation could act as a natural barrier against fire propagation, fire patch size may not continue to increase with fire intensity above a certain size. To uncover the size-intensity relationships, we matched the information on fire patch size recovered from the FRY global database (Laurent et al. 2018) based on the MODIS and MERIS sensors, with fire radiative power (FRP) using active fire pixel data from the MCD14ML dataset.

## 2 Data and Methodology

We used the FRY database containing the list of fire patches characterized by their morphological traits, including fire patch
65  size at global scale (Laurent et al. 2018). Fire patches were derived from the MERIS fire_cci v4.1 (later called FireCCI41,
Chuvieco et al. 2016) and the MCD64A1 Collection 6 (Giglio et al. 2016) burned area (BA) pixel products. The FireCCI41
product provides the pixel burn dates for the period 2005-2011 and is derived from the ENVISAT-MERIS sensor, with a
spatial resolution of 300x300m, a 3-day revisist frequency at the equator, The MCD64A1 product, derived from the MODIS
sensors, provides pixel burn dates at global scale over the period 2000-2017 with a coarser resolution (~500x500m) but a
70  more frequent revisit time (1 day at equator), The pixel burned dates are combined using a flood-fill algorithm (Archibald et
al. 2009), which is parametrized by a cut-off value. This cut-off value corresponds to the maximum time difference between
the burn date of neighbouring pixels belonging to the same fire patch. The datasets have been thoroughly compared by the
authors of the FRY database, locally compared using North America Forest Service fire patch database (Chuvieco et al.
2016) and validated landsat fire polygons in the Brazilian cerrado (Nogueira et al.2017). Fire patches in FRY are organized
75  in 8 datasets (2 surveys times 4 cut-off values), and for each individual fire patch, a set of variables, called fire patch
functional traits, are provided such as the geo-location of the patch centre, the fire patch size (later called FS, in hectares),
and different indices on fire patch morphology. Standard Deviation Ellipse (SDE) are also fitted for each fire patches, and
their half-axes and orientation are provided in longitudinal/latitudinal coordinate system. The values of the minimum and
maximum pixel burn date, and the mean burn date of the fire patch pixel are also provided.

80

Active fire pixel data from the MCD14ML dataset (Giglio et al. 2006) consists in a list of geographic coordinates of
individual active fire pixels detected by the Terra and Aqua sensors onboard the MODIS satellite for the period 2000-2017
with a resolution of 1x1km. For each pixel, the dataset provides the date and hour of burn of the active fire pixel, along with
its fire radiative power (FRP, in MW). We performed a spatio-temporal matching between active fire pixel data and all the
85  fire patches from the FRY database in order to recover the average FRP for each fire patch. To do so, we consider that an
active fire pixel belongs to a fire patch if it fulfils the two following conditions:
- The centre of the active fire pixel must be located within the SDE of the fire patch. Since the side of an active fire
pixel is 1km, we also consider that an active fire pixel located at a distance of 1km or less from the area covered by
the SDE belong to the fire patch.
90  - The detection date of the active fire pixel must lie between the minimum minus a 30 days buffer and maximum
burn date of the burned area pixels of the fire patch. The 30 days extension is used to account for the possible time
lag between the detection of an active fire pixel and its associated burned date pixels.

Once the active fire pixels belonging to each fire patch have been obtained, we compute for each patch the mean FRP value
95  of all associated pixels. In this analysis, we use FRP as a proxy of fire intensity, later called FI (Wooster et al. 2005, 2013).

The spatio-temporal matching sometimes fails to recover any active fire pixels for some fire patches. Such fire patches (~20-25% of each sample) were discarded from the analysis. We observe that the number of fire patches without attributed active fire pixels raises as the cut-off decreases (see Supplementary Tab 1). This can be explained by the fact that, for low cut-off values, a real fire event can be split by the flood-fill algorithm in different smaller fire patches. Using a shorter value for the
100  temporal buffer (10 days), slightly raises the failure rate of the matching, but had no significant impact on the results presented in this analysis.

The results presented below have been computed for each of the 8 different fire patch datasets of the FRY database. However, we will further only focus on the results obtained from the MCD64A1-derived fire patch dataset, with a cut-off
105  value of 14 days. The figures obtained for the FireCCI41 fire patch product with a cut-off of 14 days (which span the years 2005 to 2011) can be found in Supplementary. The same analysis was also performed with a cut-off value of 3 days for both MCD64A1 and FireCCI41: testing another extreme cut-off value allows us to estimate the impact of the temporal threshold parameter used to reconstruct patches by Laurent et al. (2018) on the results.

## 3 Results

110  The median FS and median FI are displayed on Figure 1. Large fire patches are located in Australia, in the grasslands of Kazakhstan, in Namibia and in Sahel, in forested regions of North America and Western Siberia, and in the Brazilian tropical savannas. These areas usually coincide with more intense fires. The highest mean FI values are also reached in South Australia, the Mediterranean Basin and in the forested areas of Western USA and boreal North America. On the contrary, fires are both smaller and less intense in croplands of North America, Europe and South East Asia, and in African savannas.
115  The relationships between the median, 25th and 75th quantiles of FS, and FI for different sub-regions defined by GFED (Giglio et al. 2013, Supplementary 1) for MCD64A1 with a cut-off value of 14 days are shown in Figure 2. The color of the dots and error bars represents the average mean of the minimum burn dates of the fire patches in each bin of FI, and the background histograms the number of fire patches in each FI bins. In all GFED regions, the number of fire patches peaks at low to intermediate FI values (~20-30 MW). This is in agreement with the observations from Luo et al. (2017), who showed
120  that fire occurrence peaked at intermediate (~30 MW) FI values. Such an agreement between fire occurrence from active fire data and the number individual of fire patches from BA is expected, since these quantities are two proxies of the number of ignitions.

Our study not only documents the effect of FI on the number of ignition, but also on fire patch size. In most of GFED
125  regions, we note that median FS and quantiles decreases once a FI threshold is reached (Figure 2). In order to smooth the estimation of this FI threshold (later called $FI_{MAX}$) above which FS seems to saturate, we interpolated a four-degree

polynomial to the data and determine the FI at the maximum median FS value of the fit. The results are displayed in Table 1 and Figure 3. For these regions, once FI gets above this regional threshold, the median and 75th quantile of FS decreases.

130 Equatorial biomes in Central America (CEAM), Equatorial Asia (EQAS) and Southeast Asia (SEAS) experience a humped relationship between FS and FI. At low FI values (30 to 80 MW), the median and quantiles of FS increases with FI and reaches a maximum value at low to intermediate FI (Table 1, Figure 3). We also identified in Figure 2 that the fire patches associated with intense fires having a FI above the regional threshold tend to occur later in the fire season. In tropical areas of Northern Hemisphere Africa (NHAF), Northern Hemisphere South America (NHSA), Southern Hemisphere Africa

135 (SHAF), Southern Hemisphere South America (SHSA), and Australia (AUST), but also in Boreal Asia (BOAS), the relationship between the median and quantiles of FS vs FI is similar. However, the maximum FS is reached at higher FI values (from 75 to 125MW) than for equatorial biomes, and the decrease following the maximum FS is more gradual. Intense fire events also appear later in the fire season for BOAS and AUST, and AUST exhibits the peculiar aspect reaching the highest FS/FI slope (9.0 ha.MW-1 compared to 0.6 to 4.4 ha.MW-1 for other regions). By contrast, in Boreal North

140 America (BONA), Temporal North America (TENA) and Europe (EURO), and Central Asia (CEAS), mean FS constantly increases with FI and only reaches a plateau at very high FI (~196 MW for BONA, ~215 MW for TENA and ~240 MW for EURO). In those temperate and boreal regions, we do not observe the humped shape relation with a decrease of FS for high FI that occurs in other GFED sub-regions (Figure 2). Middle East (MIDE) also displays a positive correlation between median FS and FI, but the statistics for intense fire events is too low to infer any significant relationship at high FI values.

145

Figure 4 shows in 1°x1° cells at global scale the month with the largest median FS, the month with the highest median FI, and the phase shift between these two months. For most African cells, the month with highest median FI is shifted between 3 to 6 months after the month with highest FS. These cells correspond to the regions where high burn area (Giglio et al. 2013) and a high density of fire patches are detected (Laurent et al. 2018). A narrower shift is observed in SEAS, northern AUST,

150 and in the cells of South America with a slightly lower number of fire patches and lower BA. In Northern America (BONA and TENA), BOAS, and central and south AUST, no shift is observed, which means that the largest fires and the most intense fires happened concomitantly during the fire season. Some cells (mainly in Sahel and eastern BOAS/CEAS) displayed a negative shift, meaning that the most intense fires happened sooner than the largest fires.

155 In each 1°x1° cells, we split the fire season into three periods: early, corresponding to the 4 months before the month with the highest BA, middle, corresponding to the peak BA month, and late fire season corresponding to the 4 months after the peak BA month. We did not split the fire patch distribution in different FI categories, because of the big asymmetry of the number of fire patches between high and low intensity fires. For each period, following the same methodology as in Laurent et al. 2018, we fitted a power law against the fire patch size distribution to estimate the power-law slope parameters $\beta_{begin}$, $\beta_{middle}$

160 and $\beta_{end}$, and displayed the resulting maps on Figure 5. The β parameters were only computed when more than 10 fire

patches are available during the considered period, to ensure a sufficient number of patches in the fit. The differences between $\beta_{end}$ and $\beta_{begin}$ are also shown in Figure 5. Highest $\beta$ values (either $\beta_{begin}$, $\beta_{middle}$ and $\beta_{end}$) happened mainly in NHAF, northern SHAF, NHSA, SHSA and SEAS, as observed in previous fire size distribution analysis (Hantson et al. 2015, Laurent et al. 2018). In these regions, we found that the value of $\beta$ is higher at the end of the fire season than at the

165   beginning, meaning that the proportion of small fires rises through the fire season. In AUST, the $\beta$ value remains constant all along the fire season, and it increases in eastern BONA, TEAS, and eastern BOAS, suggesting that later season fires are more dominated by larger fires. For other regions, the limited number of fire patches render difficult the interpretation of the evolution of $\beta$ through the fire season.


## 4. Discussion

170   Following the hypothesis from Rothermel's equation of fire spread, we used the newly delivered global fire patch database FRY to test if high FI fires propagate faster and are therefore systematically larger than low FI fires. We conclude that this hypothesis is only verified for low to intermediate FI in most of fire regions, where FI and mean FS are positively correlated. We identified biome-specific FI vs FS relationships, with FI leading to maximum FS being higher in temperate/boreal forests, followed by savannas and grasslands, and tropical areas. Following the varying constraint hypothesis (Krawchuk and

175   Moritz 2011), stating that fuel biomass availability is the main driver of fire hazard at global scale, and that fuel moisture locally modifies this fire hazard when fuel is sufficient to propagate fires, we might expect higher fire spread and energy as a function of biomass, negatively controlled by fuel moisture. Equatorial areas, with continuous high rainfall amount, then experience limited fire energy due to low fuel dryness. Along this biomass gradient, temperate and boreal forests experience a slightly longer drought period during the fire season, inducing a theoretical higher fire severity. Beside these two biomes,

180   grasslands (temperate or tropical) carry less biomass, yet still sufficient for spreading fires, and should experience the highest fire spread rate. We noted in the savanna biomes the peculiar case of AUST, with the highest values of the FRP/FS slope, twice higher than in other continents, but in accordance with local studies (Oliveira et al. 2015b). We suggest here the impact of wind speed being much higher in AUST compared to other continents (Lasslop et al. 2015).


185   However, in most fire-prone biomes, the positive relationship between FS and FI does not hold for larger and more intense fire patches (Figure 2), generally occurring later in the fire season, as previously observed in Australia by Oliveira et al. (2015a). This effect could be explained as follows: at the beginning of the fire season, when the moisture content of the fuel is still high, FRP is limited as energy is consumed for fuel moisture vaporization (Alexander 1982, Pyne et al. 1996) and consequently, fire size gets limited too. As the fuel becomes dryer along the fire season (Sow et al. 2013, Sedano and

190   Randerson 2014) fires become more intense and potentially propagate further. However, as mentioned in the introduction, the propagation of larger fires can hit some limits because of the fragmentation of the fuel matrix, due to intrinsic anthropogenic fragmentation, roads or grazing fields, which limit FS as fires became larger through the fire season. As a

result, in fire regions with fragmented vegetation, such as African savannas, SEAS or at the interface between the amazon forest and croplands of South America, a maximum mean FS is reached at intermediate FI (Figure 2). The FI threshold

195    differs however between these regions, possibly because their level of landscape fragmentation is different (Taubert et al. 2018).

If fire size would only be limited by the intrinsic structure of vegetation, we would not expect to see the decrease of the proportion of large fires the end of the fire season in fire-prone ecosystem shown in Figure 5. If the number of individual fire

200    events was already high at the beginning of the fire season, the landscape becomes even more and more fragmented by burned area scars (Oliveira et al. 2015), meaning that the limitation of fire size due to landscape fragmentation will be higher for fires ignited later in the fire season. As a consequence, this mechanism may explain why the correlation between FI and FS becomes negative in Figure 2 during the late fire season in NHAF, NHSA, CEAM, EQAS and SEAS, and why $\beta_{end}$ is higher than $\beta_{begin}$. This limitation of fire size for intense fires in those regions, possibly due to the feedback between fire and

205    fuel connectivity at landscape level, is in line with the results obtained from Mondal and Sukumar (2016) relating the effects of recent past fires on fire hazard in dry tropical forests, and otherwise theoretically approached from the percolation model applied to wildfires by Archibald et al. (2012). This model shows that the amount of BA is maximized when both the fire spread probability and the fuel matrix connectivity are high. BA dramatically drops if fire spread probability is too low (such as in the beginning of the fire season) or if the fuel array connectivity becomes too low (such as in the end of the fire season).

210    Particularly, the percolation model shows that BA dropped dramatically once 50-60% of the available fuel has burned, which is close to the maximum percentage of BA detected by both MCD64A1 and FireCCI41 products (Giglio et al. 2013, Chuvieco et al. 2016). The IFOI hypothesis, proposed by Luo et al. (2017) to explain why fire occurrence is limited by fire intensity, can be interpreted as a direct consequence of percolation theory applied to fire-prone ecosystems.

215    For regions where fire events are less frequent, such as in BONA, TENA and EURO (Figure 2), there is no significant limitation of fire spread and fire size, suggesting that the fragmentation of landscape either from land use or from early season burn scars does not limit fire spread (Owen et al. 2012). Fire size remains positively correlated with fire intensity all along the fire season. Moreover, the 75th quantiles for BONA and TENA is higher than for tropical regions (except AUST), most probably because tree species in BONA and TENA are more flammable (e.g. spruce) and because crown fires are more

220    frequent, and because these ecosystems experience an actual drought period compared to the tropics where rainfalls occur all year long. They can therefore propagate further than ground fire and fire resistant species found in savannas and woodlands in semi-arid tropical regions. In BOAS the relationship between FS and FI is different from the one observed in BONA and TENA. This could be a result from the less flammable vegetation and the highest number of ground fires (Kasischke and Bruhwiler 2003). Moreover, BA detection of surface fires (and consequently, fire patch characterization) is known to be

225    difficult in boreal Asia, and numerous discrepancies have been observed between the BA products obtained from different moderation resolution sensors (Chuvieco et al. 2016).

The median FS is globally lower for the datasets generated from FRY with smaller cut-off value (see Supplementary 1 and 2), because big fire patches tend to be split in smaller patches for lower cut-off values, reducing the average fire patch size.

230 The median FS is also lower for the FireCCI41derived datasets, due to its ability to detect smaller patches from its better spatial resolution. Changing the survey or the cut-off value does not impact the global distribution of large and small fire patches. Reducing the cut-off to 3 days does not change the observed relationship between FS and FI. The results obtained from the dataset derived from FireCCI41 follows the same trend, but for some GFED regions (TENA, EURO, NHSA, AUST) the seasonality is shifted one month later than for MCD64A1. Reducing the cut-off values lowers the temporal shift

235 observed on Figure 4 at global scale (Supplementary 3 and 4), but the global distribution of the shift is conserved. Similarly, FireCCI41 yields smaller shifts than for MCD64A1, but with the same spatial distribution.

Fire danger index has been constantly increasing during the last 50 years (Jolly 2015) and could impact fire season length and/or intensity all over the world. An increase of drought intensity in fire prone environment could yield to more intense

240 fire events, yielding larger burned area patches for each fire event. However, if the progressive fragmentation of landscape through the fire season limits fire size, then it can be expected that a longer fire season would only have a limited impact on the increase of BA in these regions. In the same way but on a longer time scale in less fire prone regions, previous large fires have been shown to limit FS in the recent timeframe in western US (Haine et al 2013), and previous landscape biomass composition, as a result of fire history, is a major factor affecting fire severity in boreal forests (Whitman et al. 2018). On the

245 contrary, in regions where the quasi-linear relationship between fire size and FRP is valid even for high FRP, a longer fire season could dramatically increase burn area, particularly in North America and Europe (Gillett et al. 2004, Turetsky et al. 2011). This hypothesis does not account for the impact of increased severity of fire damage to the vegetation in these ecosystems, and its feedback on fire propagation and occurrence. Our results are consistent with those of Andela et al. 2017, who showed that, contrary to what would be expected from the rise of the fire danger index, BA tends to decline at global

250 scale (25% loss between 1998 and 2015). This decline is especially strong in savannas and grasslands, because of agricultural expansion, which results in a reduction of burnable area and a more fragmented landscape. Landscape fragmentation is also a tool used for fire management. Indigenous burning practices in West Africa promotes early burning and therefore landscape fragmentation in order to limit large and intense fire events which could occur at the end of the fire season (Laris and Wardell 2006, Archibald 2016). Similarly, US forest services used artificial fuel-breaks to fragment the

255 landscape and limit fire size (Green 1977, Agee et al. 2000), as well as fire intensity (Ager et al. 2017).

Some DGVM fire modules explicitly simulate BA as the product of individual successful fire ignitions with mean fire size (Thonicke et al. 2010, Yue et al. 2014). In these models, fire size usually depends on wind speed, fuel bulk density and fuel load. It is common than BA saturates toward the end of the drought season because of the reduction of the available fuel load

260 due to burning by preceding fires, but this mechanism does not account for landscape fragmentation (due either to land use

Biogeosciences

Discussions

fragmentation or progressive fragmentation by fires). The LPJ-LMFire v1.0 (Pfeiffer et al. 2013), a modified version of the Spitfire module for pre-industrial global biomass burning, accounted for passive fire suppression due to landscape fragmentation. Further refining of process-based fire modules would require extensive comparison with fire patch data rather than raw BA.

## 5. Conclusion

We characterized for the first time the actual relationship between fire size and fire intensity using a combination of fire patch size and active fire datasets at global scale. We found that in most fire-prone ecosystems, fire size increases with fire intensity only at low fire intensity, reaches a threshold at intermediate intensity, and then starts to decrease. On the contrary, in temperate and boreal forests, FS and FI are proportional even for high fire intensity. This behavior is observed for both MCD64A1 and FireCCI41 products, and for all cut-off values used for fire patch reconstruction. We suggested that the FI threshold value is driven by drought severity, available biomass, the fragmentation of the landscape, and the feedback between fuel connectivity and burn area during the fire season. This fragmentation hypothesis is consistent with the percolation model applied to fire spread. The fragmentation hypothesis should be further tested with higher resolution BA datasets, combined with fine temporal resolution land cover datasets characterizing the landscape fragmentation, associated with temporally varying fuel moisture data, and further considered in fire-DGVM models. Additional information as fire shape complexity and elongation from the FRY database should bring substantial information to assert our conclusions.

**References**

Agee, J. K, Bahro, B., Finney, M. A., Omi, P. N., Sapsis, D. B., Skinner, C. N., van Wagtendonk, J. W., Weatherspoon, C. P.: The use of shaded fuelbreaks in landscape fire management, Forest Ecology and Management, 127(1-3), 55-66, 2000.

Ager, A.A., Barros, A.M.G., Preisler, H.K., Day, M.A., Spies, T.A., Bailey, J.D., Bolte, J.P. Effects of accelerated wilfire on future fire regimes and implications for the United States federal fire policy. Ecology and Society, 22(4), 12, 2017.

Alexander, M.E.: Calculating and interpreting forest fire intensities. Can. J.Bot. 60: 349-357, 1982.

Andela, N., Morton, D. C., Giglio, L., Chen, Y., van der Werf, G. R., Kasibhatla, P. S., DeFries, R. S., Collatz, G. J., Hantson, S., Kloster, S., Bachelet, D., Forrest, M., Lasslop, G., Li, F., Mangeon, S., Melton, J. R., Yue, C., and Randerson, J. T.: A human-driven decline in global burned area, Science, 356, 1356–1362, 10.1126/science.aal4108, 2017.

Archibald, S. and Roy, D. P.: Identifying individual fires from satellite-derived burned area data. in III-160-III-163 (IEEE). doi:10.1109/IGARSS.2009.5417974, 2009.

Archibald, S., Scholes, R. J., Roy, D. P., Roberts, G. and Boschetti, L.: Southern African fire regimes as revealed by remote sensing. International Journal of Wildland Fire 19, 861, 2010.

290    Archibald, S., Staver, A. C. and Levin, S. A.: Evolution of human-driven fire regimes in Africa. Proceedings of the National Academy of Sciences 109, 847–852, 2012.

Archibald, S., Lehmann, C. E. R., Gomez-Dans, J. L. and Bradstock, R. A.: Defining pyromes and global syndromes of fire regimes. Proceedings of the National Academy of Sciences 110, 6442–6447, 2013.

Archibald S.: Managing the human component of fire regimes: lessons from Africa. Phil. Trans. R. Soc. B 371:20150346, 295    http://dx.doi.org/10.1098/rstb.2015.0346, 2016

Aragão, L. E. O. C. et al.: 21st Century drought-related fires counteract the decline of Amazon deforestation carbon emissions. Nature Communications 9, 2018.

Barrett, K. and Kasischke, E. S.: Controls on variations in MODIS fire radiative power in Alaskan boreal forests: Implications for fire severity conditions. Remote Sens. Environ., 130, 171-181, https://doi.org/10.1016/j.rse.2012.11.017, 300    2013.

Baker, W. L.: Restoration of Landscape Structure Altered by Fire Suppression. Conservation Biology, 8: 763–769. doi:10.1046/j.1523-1739.1994.08030763.x, 1994.

Bond, W. J., and Keeley, J. E.: Fire as a global 'herbivore': The ecology and evolution of flammable ecosystems, Trends Ecol. Evol., 20(7), 387–394, 2005.

305    Bowman, D. M. J. S. and Balch, J. K.: Fire in the Earth System. Science 324, 481–48, 2009.

Cary, G.J. et al.: Comparison of the sensitivity of landscape-fire-succession models to variation in terrain, fuel pattern, climate and weather. Landsc. Ecol. 21(1), 121-137, 2006.

Chuvieco, E. et al.: A new global burned area product for climate assessment of fire impacts: A new global burned area product. Global Ecol. and Biogeography 25, 619–629, 2016.

310    Crutzen, P. J. et al.: Biomass Burning as a Source of Atmospheric Gases $CO_2$, $H_2$, $N_2O$, NO, $CH_3Cl$ and COS, Nature, 282(5736), 253–256, 1979.

Flannigan, M. D., Krawchuk, M. A., de Groot, W. J., Wotton, B. M., and Gowman, L. M.: Implications of changing climate for global wildland fire, Int. J. Wildland Fire, 18(5), 483–507, 2009.

Gillett, N. P. et al.: Detecting the effect of climate change on Canadian forest fires. Geophysical Research Letters 31, 2004.

315    Giglio, L., Csiszar, I., and Justice, C. O.: Global distribution and seasonality of active fires as observed with the Terra and Aqua MODIS sensors. Journal of Geophysical Research, 111, G02016, doi:10.1029/2005JG000142, 2006

Giglio, L., Randerson, J. T. and van der Werf, G. R.: Analysis of daily, monthly, and annual burned area using the fourth-generation global fire emissions database (GFED4): Analysis Of Burned Area. Journal of Geophysical Research: Biogeosciences 118, 317–328, 2013.

320    Giglio, L., Schroeder, W., and Justice, C.: The collection 6 MODIS active fire detection algorithm and fire products, Remote Sens. Environ. 178, 31–41, 2016.

Green, L.: Fuelbreaks and other fuel modification for wildland fire control. Agricultural Handbook No. 499, 1977.

Haire, S.L., McGarigal, K., Miller, C. Wilderness shapes contemporary fire size distributions across landscapes of the western United States. Ecosphere, 4 (1), 15. 2013.

325 Hantson, S., Pueyo, S. and Chuvieco, E.: Global fire size distribution is driven by human impact and climate: Spatial trends in global fire size distribution. Global Ecology and Biogeography 24, 77–86, 2015.

Hantson, S. et al.: The status and challenge of global fire modelling. Biogeosciences 13, 3359–3375, 2016.

Ichoku, C., Giglio, L., Wooster, M. J., and Remer, L. A.: Global characterization of biomass-burning patterns using satellite measurements of fire radiative energy, Remote Sensing of Environment, 112(6), 2950-2962, 2008.

330 Jolly, W. M. et al.: Climate-induced variations in global wildfire danger from 1979 to 2013. Nature Communications 6, 2015.

Kasischke, E.S. and Bruhwiler, L.P.: Emissions of carbon dioxide, carbon monoxide and methane from boreal forest fires in 1998. Journal of geophysical research 108(D1): 8146. DOI:10.1029/2001JD000461, 2003.

Krawchuk, M.A. and Moritz, M.A.: Constraints on global fire activity vary across a resource gradient. Ecology. 92:121-132, 2011.

335 Krawchuk, M. A., Moritz, M. A., Parisien, M.-A., Van Dorn, J. and Hayhoe, K.: Global pyrogeography: The current and future distribution of wildfire, PLoS One, 4(4), e5102, 2009.

Laris, P. and Wardell, D. A.: Good, bad or 'necessary evil'? Reinterpreting the colonial burning experiments in the savanna landscapes of West Africa. The Geographical Journal, 172(4), 271–290, 2006.

Lasslop G., Hantson S., and Kloster S.: Influence of wind speed on the global variability of burned fraction a global fire

340 model's perspective. Int. J. wild. Fire 24(7): 989-1000, 2015).

Laurent, P. et al.: FRY, a global database of fire patch functional traits derived from space-borne burned area products. Sci. Data 5:180132 doi: 10.1038/sdata.2018.132, 2018.

Luo, R., Hui, D., Miao, N., Liang, C. and Wells, N.: Global relationship of fire occurrence and fire intensity: A test of intermediate fire occurrence-intensity hypothesis: Fire Occurrence-Intensity Relationship. Journal of Geophysical Research:

345 Biogeosciences 122, 1123–1136, 2017.

Mondal, N. and Sukumar, R.: Fires in seasonnaly dry tropical forest: testing the varying constraints hypothesis acriss a regional rainfall gradient. Plos one. 11(7): e0159691.doi:10.1371/journal.pone.0159691, 2016.

Mouillot, F. et al.: Ten years of global burned area products from spaceborne remote sensing—A review: Analysis of user needs and recommendations for future developments. Int. J. of Appl. Earth Obs. and Geoinf. 26, 64–79, 2014.

350 Oliveira, S. L. J. et al.: Ecological Implications of Fine-Scale Fire Patchiness and Severity in Tropical Savannas of Northern Australia. Fire Ecology 11, 10–31, 2015a.

Oliveira, S.L.J., Maier, S.W., Pereira, J.M.C., Russell-Smith, J. Seasonal differences in fire activity and intensity in tropical savannas of northern Australia using satellite measurments of fire radiative power. Int. J. Wild. Fire 24 (2), 249-260, 2015b.

Owen, F. P., Russel-Smith, J., and Watt, F.: The influence of prescribed fire on the extent of wildfire in savanna landscapes of

355 western Arnhem Land, Australia, International Journal of Wildland Fire, 21 (3), 297-305, 2012.

Nogueira, J.M.P., Ruffault, J., Chuvieco, E., Mouillot, F. 2017. Can we go beyond burned area in the assessment of global remote sensing products with fire patch metrics? Remote Sens. 9 (1), 7, 2017.

Pausas, J. G., and Ribeiro, E.: The global fire-productivity relationship, Global Ecol. Biogeogr., 22(6), 728–736, 2013.

Pfeiffer, M., Spessa, A. and Kaplan, J.O.: A model for global biomass burning in preindustrial time: LPJ-LMfire (v1.0),
360    Geosci. Model Dev., 6, 643–685, 2013.

Pyne, S. J, Andrews, P. L. and Laven, R. D.: Introduction to Wildland Fire. Wiley, 1996.

Rothermel, R. C.: A mathematical model for predicting fire spread in wildland fuels. USDA Forest Services. Research Paper INT-115, 1972.

Rabin, S. S., Melton, J. R., Lasslop, G., Bachelet, D., Forrest, M., Hantson, S., Kaplan, J. O., Li, F., Mangeon, S., Ward, D.
365    S., Yue, C., Arora, V. K., Hickler, T., Kloster, S., Knorr, W., Nieradzik, L., Spessa, A., Folberth, G. A., Sheehan, T., Voulgarakis, A., Kelley, D. I., Prentice, I. C., Sitch, S., Harrison, S., and Arneth, A.: The Fire Modeling Intercomparison Project (FireMIP), phase 1: experimental and analytical protocols with detailed model description, Geoscientific Model Development, 10, 1175–1197, 10.5194/gmd-10-1175-2017, 2017.

Scott, A. C. et al.: Fire on Earth: An Introduction, Wiley-Blackwell, 434 pages, 2014.

370    Sedano, F. and Randerson, J. T.: Multi-scale influence of vapor pressure deficit on fire ignition and spread in boreal forest ecosystems. Biogeosciences 11, 3739–3755, 2014.

Sow, M., Mbow, C., Hely, C., Fensholt, R. and Sambou, B.: Estimation of herbaceous fuel moisture content using vegetation indices and land surface temperature from MODIS data. Remote Sensing 5(6): 2617-2638, 2013.

Tang, W., and Arellano Jr., A. F.: Investigating dominant characteristics of fires across the Amazon during 2005–2014
375    through satellite data synthesis of combustion signatures, J. Geophys. Res. Atmos., 122, 1224–1245, doi:10.1002/2016JD025216, 2017.

Taubert, F. et al.: Global patterns of tropical forest fragmentation, Nature 554, 519–522, 2018.

Thonicke, K. et al. The influence of vegetation, fire spread and fire behaviour on biomass burning and trace gas emissions: results from a process-based model. Biogeosciences 7, 1991–2011, 2010.

380    Turetsky, M. R. et al.: Recent acceleration of biomass burning and carbon losses in Alaskan forests and peatlands. Nature Geoscience 4, 27–31, 2011.

Turner, M.G.: Landscape ecology: the effect of pattern on process. Annual Review of Ecology and Systematics 20:171–197, 1989.

Wagner, C. V.: A simple fire-growth model. The Forestry Chronicle 45, 103–104, 1969.

385    Whitman, E., Parisien, M.A., Thompson, D.K., Hall, R.J., Skakun, R.S., Flannigan, M.D. Variability and drivers of burn severity in the northwestern Canadian boreal forest. Ecosphere 9 (2), e02128, 2018.

Wooster, M. J., Roberts, A. F., Perry, G. L. W. and Kaufman, Y. J.: Retrieval of biomass combustion rates and totals from fire radiative power observations: FRP derivation and calibration relationships between biomass consumption and fire radiative energy release. Journal of Geophysical Research 110, 2005.

390   Wooster, M. J., Roberts, G., Smith, A. M. S., Johnston, J., Freeborn, P., Amici, S. and Hudak, A. T.: Thermal Remote Sensing
      of Active Vegetation Fires and Biomass Burning Events. Thermal Infrared Remote Sensing. C. Kuenzer and S. Dech,
      Springer Netherlands. 17:347-390, 2013.

      Yue, C. et al. Modelling the role of fires in the terrestrial carbon balance by incorporating SPITFIRE into the global
      vegetation model ORCHIDEE – Part 1: simulating historical global burned area and fire regimes. Geosci. Mod.
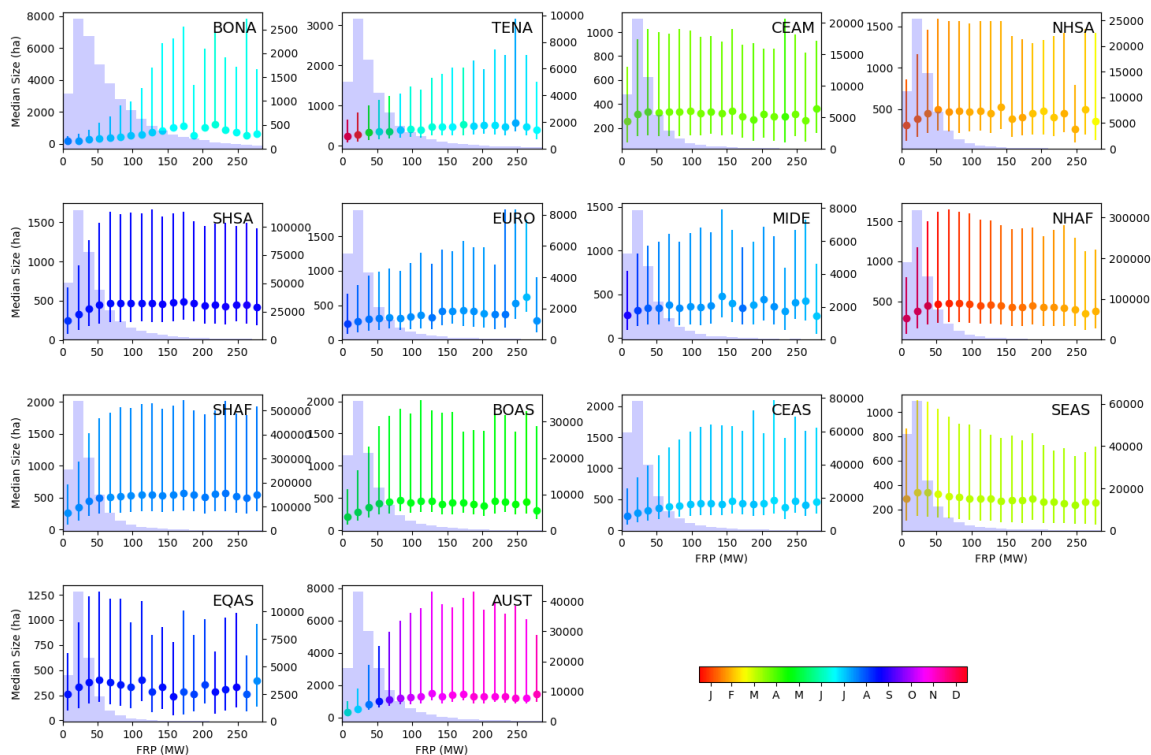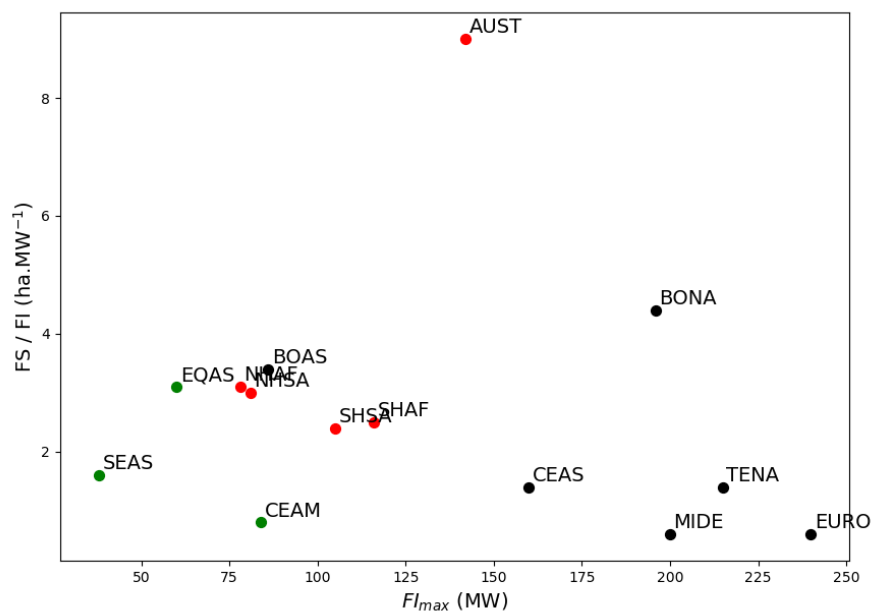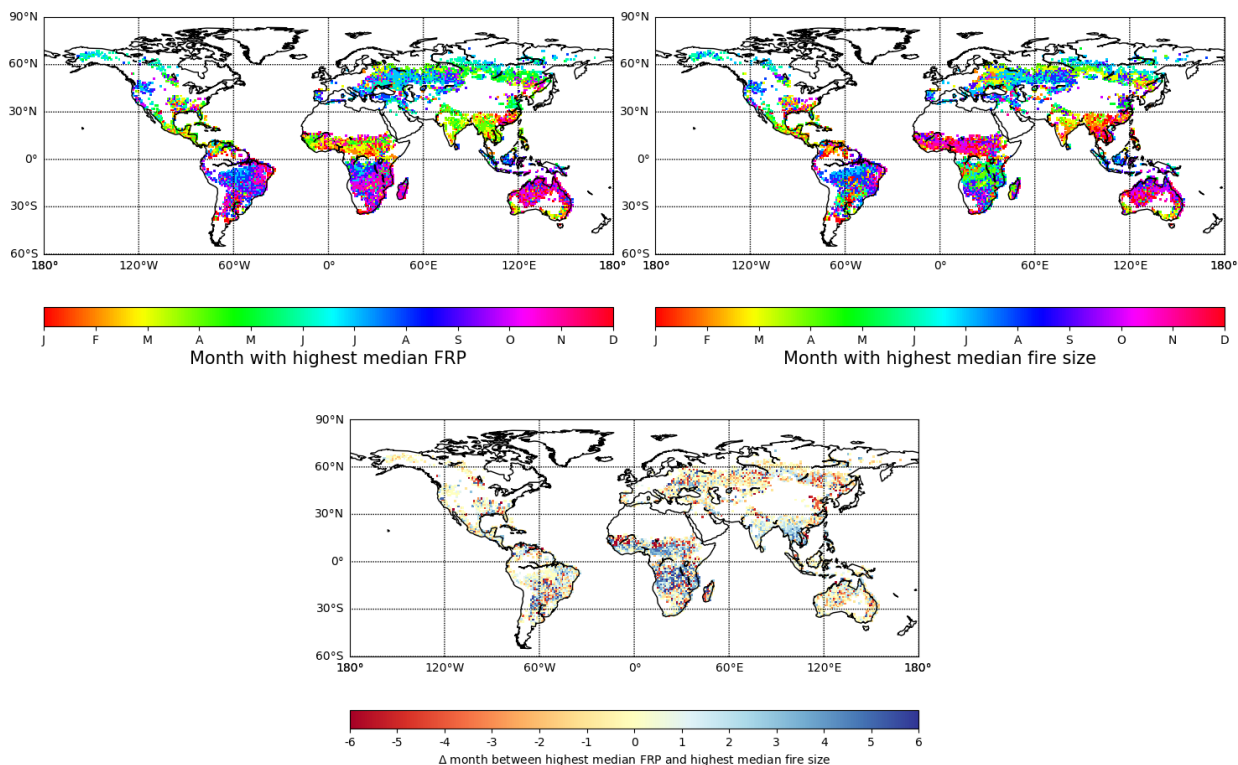395   Development 7, 2747–2767, 2014.

**Figure 1: Mean fire size FS (patch area in ha) and fire intensity FI using FRP as proxy (in MW) for MCD64A1 with a cut-off of 14 days in the patch reconstruction algorithm.**

**Figure 2: Median FS vs FI for different GFED regions. The error bars represent the 25th and 75th quantiles of the FS distribution. The color of the dots and error bars represent the mean burn date of fire patches in each FI bin.**

Biogeosciences
Discussions

Open Access



**Figure 3: FI threshold (FI$_{MAX}$, in MW) vs slope between FI and median FS (in ha.MW$^{-1}$) before FI$_{MAX}$ for the different GFED subregions. Green dots represent GFED subregions dominated by tropical forests, red dots the subregions dominated by grasslands/savannas and black dots the subregions dominated by temperate/boreal forests.**

405

**Figure 4: Month with highest median FRP (top left), highest median FS (top right), and the difference between the two (bottom). In blue cells, the month with the largest fires events happen before the month with the most intense fires. In red cells, the month with the largest fires events happen before the month with the most intense fires. In yellow cells, the months with the largest fires and with the most intense fires are the same.**
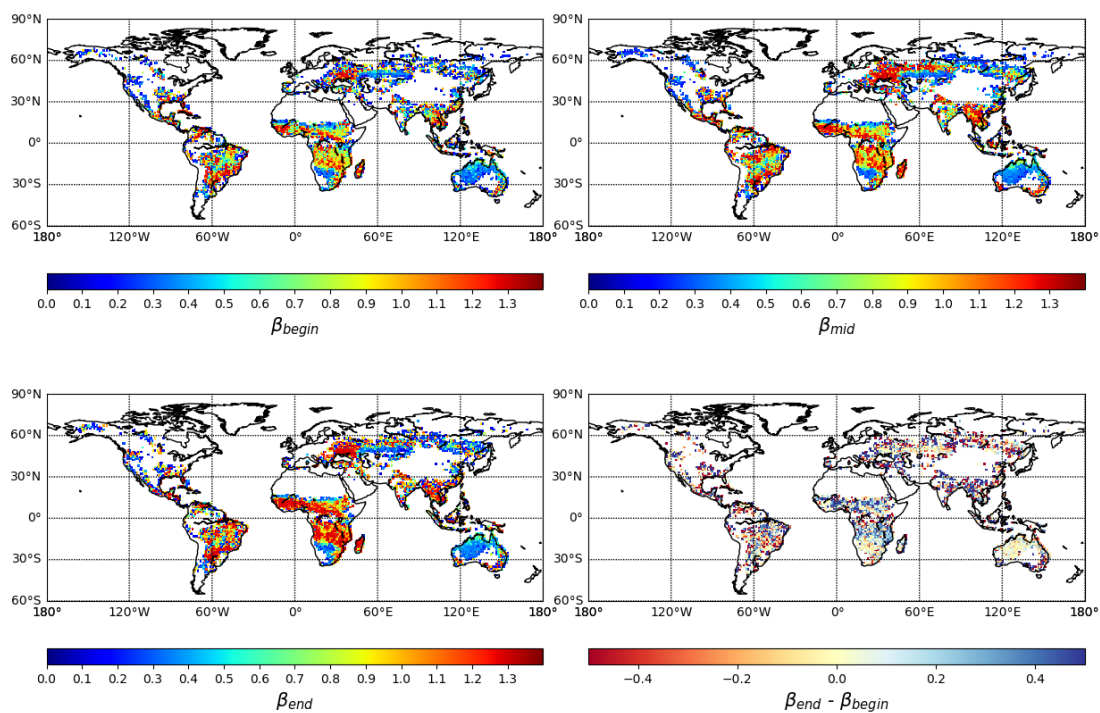
**Figure 5: Value of the log-log scale slope of the fire size distribution at the beginning of the fire season, beta (4 months before the month with the highest amount of BA), in the middle of the fire season (corresponding to the month with the highest BA) and at the end of the fire season (4 months after the month with highest BA).**

415

| GFED Region | FI at maximum size (MW) | Slope of the FI vs median FS relationship before max FS (ha.MW$^{-1}$) |
|---|---|---|
| BONA | 196 | 4.4 |
| TENA | 215 | 1.4 |
| CEAM | 84 | 0.8 |
| NHSA | 81 | 3.0 |
| SHSA | 105 | 2.4 |
| EURO | 240 | 0.6 |
| MIDE | 200 | 0.6 |
| NHAF | 78 | 3.1 |
| SHAF | 116 | 2.5 |
| BOAS | 86 | 3.4 |
| CEAS | 160 | 1.4 |
| SEAS | 38 | 1.6 |
| EQAS | 60 | 3.1 |
| AUST | 142 | 9.0 |

**Table 1 : Value of the FI threshold at maximum median FS, and the slope of FS vs FI before the threshold value for different GFED regions.**